Communications in Physics, Vol. 21, No. 2 (2011), pp. 169-178

FEASIBILITY STUDY OF DIRECT MEASUREMENT OF STELLAR REACTION ^{22}Mg$(\alpha, p)^{25}$Al

NGUYEN NGOC DUY
Dong Nai University
LE HONG KHIEM
Institute of Physics, VAST

Abstract. *The stellar reaction $^{22}Mg(\alpha,p)^{25}Al$ plays an important role for understanding the nucleosynthesis of stars. It has never investigated yet. We are planning to study this reaction in environment of X-rays burst with temperature T9 = 1÷3 GK using invert kinematics and thick target method. This paper shows a design for direct investigation of this reaction by simulation method. This design is necessary for experimental setup and for confirmation of the feasibility of the experiment.*

I. INTRODUCTION

Our purpose focuses on the study of nuclear reactions and structure that are of importance to understanding explosive nucleonsynthesis in X-ray bursts and novae. The synthesis of light and intermediate-mass elements can take place through radiative proton captures on unstable nuclei during explosive stellar events. In the past, the seminal idea was codified [1,2]. This idea was that essentially of all the elements were made by thermonuclear burning in stars. The processes were called stellar nucleosynthesis. Later, astronomical observations [3, 4] suggested that the elements were formed by some other process early in cosmological history, perhaps in the Big Bang itself. From Big Bang, the nucleosynthesis passes through many processes from proton-proton chain, rapid proton capture (rp-process), αp-process,... to p-process for synthesizing heavy elements (A$\geq$74). These processes involve the majority of the nuclei between the proton and the neutron drip line up to a maximum mass number set by the endpoint of the rp-process. In this scenario, the rp-process during X-ray bursts (and maybe during stable hydrogen burning as well) plays a central role as it directly determines one of the key observables, the observed X-ray bursts, and because it sets the initial composition for all the deeper processes.

For lighter nuclei (up to mass around 40), at the high temperature (about 6 x 10^8 K) and high density, the basic rp-process is altered by (α,p) reaction that bridge the β+ decay associated with "waiting point". From that point on nuclear energy generation is dominated by α-particle capture consisting of a series of (α, p) and (p,γ) reaction. Two prominent reaction chains emerge. One involves the burning of ^{15}O to ^{25}Si and the other involves the burning of ^{14}O to ^{24}Si and ^{26}Si, which consists of the ^{22}Mg(α, p)^{25}Al reaction. Depending on the peak temperature reached in a particular burst, the final αp-process can extend up to Sc, mainly through the sequence:

$^{14}O(\alpha,p)^{17}F(p,\gamma)^{18}Ne(\alpha,p)^{21}Na(p,\gamma)^{22}Mg(\alpha,p)^{25}Al(p,\gamma)^{26}Si(\alpha,p)$ $^{29}P(p,\gamma)^{30}S(\alpha,p)^{33}Cl(p,\gamma)^{34}Ar(\alpha,p)^{37}K(p,\gamma)^{38}Ca(\alpha,p)^{41}Sc$.

Our present understanding of the energy generation and nucleosynthesis in Type I X-ray bursts indicates that the overall behavior of the burst's luminosity curve and the reaction path is related to waiting point nuclei in the αp-process, namely, ^{22}Mg, ^{26}Si, ^{30}S, and ^{34}Ar [5]. The (α,p)-rates for these nuclei are currently unknown and should be obtained experimentally.

Among the isotopes synthesized in novae, two radioactive species have generated particular astrophysical interest: ^{22}Na and ^{26}Al. These isotopes relate to the double-peaked type I X-ray burst observed by HEAO-C satellite in 1982 and 1984. Their beta decays lead to the emission of the 1.275 MeV and 1.809 MeV gamma rays, respectively [6]. The stellar reaction $^{22}Mg(\alpha,p)^{25}Al$ plays an important role of either explanation of those gamma rays line in cosmic spectra or investigation of synthesis of ^{25}Al in stars. The other motivation is to significantly advance knowledge of the nuclear level structure of ^{26}Si. Indeed there is limited information concerning even the position of states in the compound system ^{26}Si at and above the α-particle threshold energy as seen in Fig. 1. Also from strictly nuclear physics view point, the study of the structure of exotic nuclei has gained significant importance.

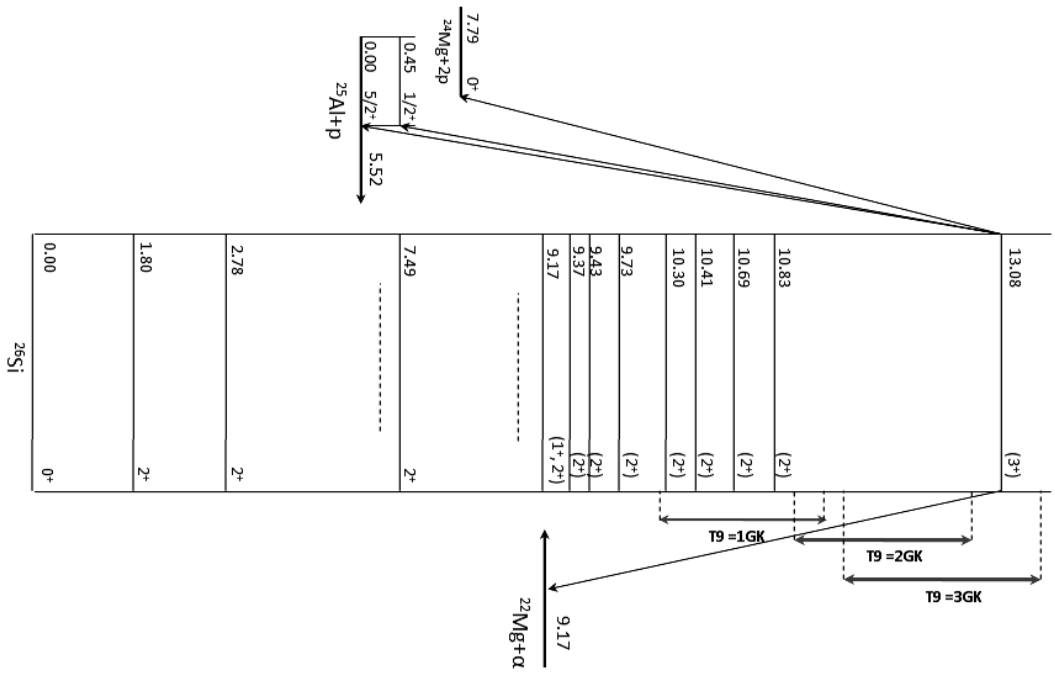

Fig. 1. Levels scheme of ^{26}Si.

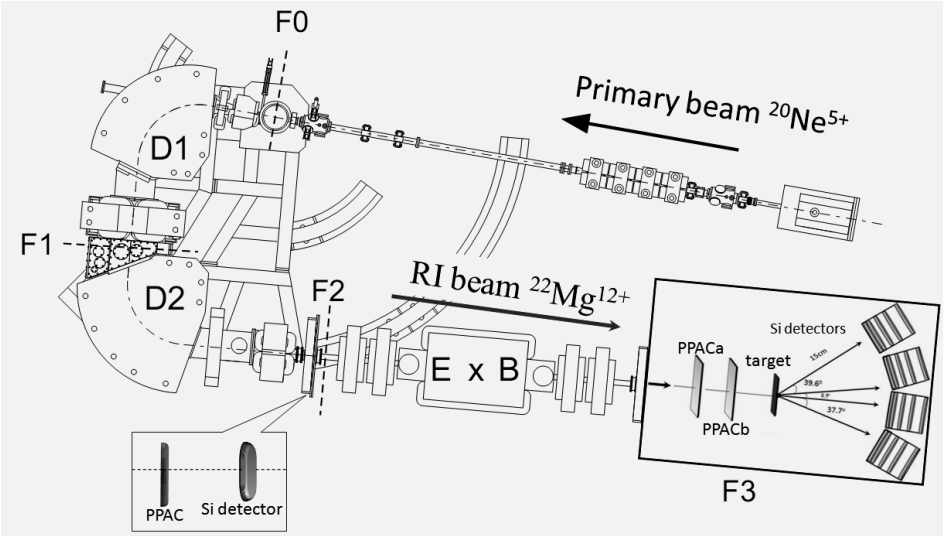

Fig. 2. The CRIB spectrometer.

In the past, it was difficult for studying stellar nuclear reactions because dificulties of prduction of the unstable isotopes with the very short life time as well as the special measurement techniques are needed. Since the advent of radioactice beam facilities together with the rapid development of measurement techniques including the modern magnetic spectrometers, it is feasible to perform these reactions. These open up an invaluable means to experimentally access nuclei for which very little is known at present.

This paper presents a practical experimental design for direct investigation of ^{22}Mg$(\alpha, p)^{25}$Al reaction using the CRIB for production of radioactive beam ^{22}Mg ($J^{\pi} = 0^{+}$, $\tau = 3.857$ s). The study will cover an energy region from 1.1 MeV to 4.2 MeV in the center of mass frame of the ^{22}Mg+α system, which corresponds to Gamow window with an assumption of the temperature from 1GK to 3GK of X-ray burst. Our experiment is expected to yield data with a high accuracy, a high energy resolution as well as with detailed angular distribution information. So far, this reaction has not been studied yet [8]. We planed to perform this reaction using CRIB spectrometer [7] at the Center for Nuclear Study of the University of Tokyo, which was installed at RIKEN, Japan. The ^{22}Mg radioactive beam will be produced via ^{3}He(^{20}Ne,^{22}Mg)n primary reaction in inverse kinematics. The various computer codes such as Lise++, NON-SMOKER and CRIB optimizer were used for simulation.

II. DESIGN EXPERIMENT OF ^{22}Mg$(\alpha, p)^{25}$Al REACTION

II.1. The CRIB spectrometer

The structure of double achromatic CRIB spectrometer is presented in Fig3. The main components of CRIB are two dipole magnets D1 and D2 and several quadrupole magnets in between. The CRIB can produce low energy (< 10 MeV/u) radioactive ion

(RI) beam by the in-flight method, from the stable nuclei beam accelerated at an AVF cyclotron (K=70). Using two dipole magnets, produced particles are separated, and we can obtain various kinds of radio isotopes as secondary beams A Wien filter, installed downstream of the two dipole magnets, gives further separation according to the velocity of the beam. With the latest technology of the heavy-ion source and accelerator, this facility can provide an intense and good-quality RI beam, which is applicable for various fields of physics research, especially for the nuclear astrophysics.

In order to increase the purity of the beam, the Wien Filter will be used after F2. The Wien filter can separate the beam by the horizontal electric field and vertical magnetic field. The forces from the electric and magnetic field balance at a fixed velocity, for given B and E fields (since qE=qvB). Therefore, we are able to set the B and E fields so that only the beam with a desired velocity can go straight in the Wien filter. The Wien filter can make a velocity dispersion of 0.43 cm/% at F3, with high voltages of ± 100 kV. When we have a separation of few cm between the necessary beam and unnecessary beam (and the unnecessary beam is not too strong), we can completely eliminate the unnecessary beam by a movable slit located after the Wien Filter. There is a large vacuum chamber at F3 for the detectors and targets, in the downstream of the Wien filter. This chamber is called scattering chamber.

II.2. The beam production reaction

The beam production reaction will be performed at F0 chamber using a thick gas target ^{3}He in inverse kinematics. The total center-of-mass energy $E_{cm}$of the system (^{20}Ne + ^{3}He) will be in the range from 13.1 MeV to 13.89 MeV, which corresponds to energy of $^{22}Mg^{12+}$ in the range from 0.49 ÷ 0.58 MeV/u. This energy region corresponds to Gamow window in X-rays burst environment with temperature T_9 = 1÷3 GK. Therefore, the incident beam $^{20}Ne^{5+}$ should be accelerated by the AVF accelerator up to the energy in the range from 5.7 ÷ 5.9 MeV/u. The best suitable primary reaction shoub be ^{3}He(^{20}Ne, ^{22}Mg)n because it has a large cross section. In order to estimate the ^{22}Mg beam intensity, the production cross section was extrapolated based on the experimental data obtained from ^{20}Ne(^{3}He, n)^{22}Mg reaction with the center-of-mass energy of 4.57, 6.76, 7.67, 8.12 and 20.6 MeV [14, 15, 16, 17]. By extrapolation, we obtained the cross section σ = 17 ÷ 23 mb corresponding to E_{cm} = 13 ÷ 15 MeV. The result is presented in Fig. 3.

The ^{3}He gas production target of 8 cm thickness is confined by the entrance and exit Havar foil windows with the thickness of 2.5μm. The temperature of gas is 77 K and the pressure is 300 Torr. The density of gas therefore is 0.0001804 g/cm^3. We have to choose an optimal energy of the primary beam in order to maximize the cross section of the production of ^{22}Mg. Futhermore, the energy straggling through target must be kept to be smaller than 1%. According to the momentum acceptance of CRIB, the energy spread of 2 MeV (FWHM) of primary beam after the production target was estimated. Therefore, we are able to obtain the secondary beam which satisfies the requirement of energy resolution of the (α,p) reaction (100 keV in center-of-mass system) as presented in Fig. 4.

The momentum of the $^{22}Mg^{12+}$ secondary beam will be analyzed by the dipole magnet D1. After D1, the beam will reach the momentum dispersive focal plane F1

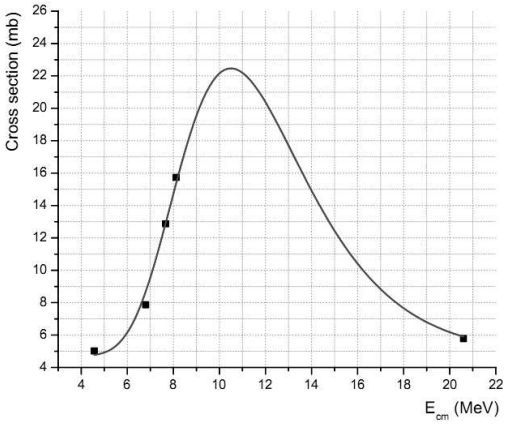

Fig. 3. Cross section curve of ^{20}Ne$(^3$He$, n)^{22}$Mg.

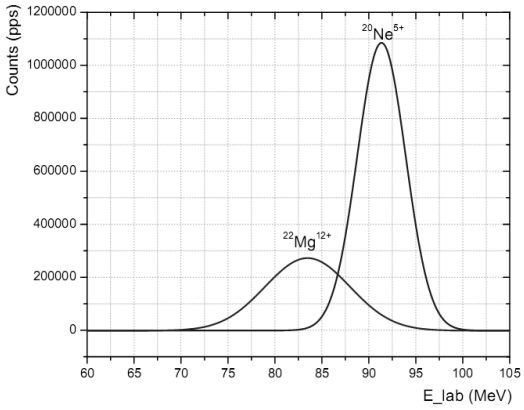

Fig. 4. The energy distribution of ^{22}Mg^{12+} and ^{20}Ne^{5+} in the production target.

where the interested secondary beam will be selected by a slit. The beam is focused achromatically at the second focal plane F2. Fig. 5 presents the simulated results for particle identification of the beam at F2 by the ΔE-TOF method, where TOF is time-of-?ight measured between RF signal from cyclotron and a Parallel-Plate Avalanche Counters (PPAC) at F2 while ΔE indicates the energy loss measured by a Si detector located downstream of this PPAC. It can be seen from the figure that the particles can be clearly identified at F2. Consequently, the desired beam ^{22}Mg^{12+} will be separated from other contaminants such as ^{21}Na, ^{18}Ne, ^{18}F, ^{14}O ,...

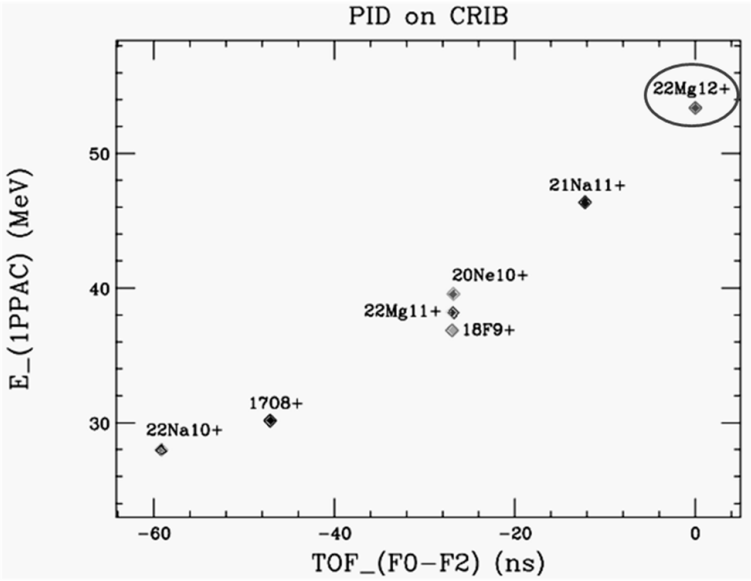

Fig. 5. Particle identification of beam time with Bρ = 0.449 Tm.

The value of $B\rho$ will be set at 0.449 Tm which corresponds to the central $B\rho$ value of $^{22}Mg^{12+}$. The difference of total energy between $^{20}Ne^{5+}$ and $^{22}Mg^{12+}$ is 15.6 MeV, therefore the difference in position between $^{20}Ne^{5+}$ and $^{22}Mg^{12+}$ is $\Delta x = 5$ cm. This difference allows us to use the slit for selection of $^{22}Mg^{12+}$ without the major contaminants. Further selection of the beam will be done by using Wien filter located right after F2. According to our simulation, the $^{22}Mg^{12+}$ will have a high purity at F3. Assuming the transmission through dipole magnets and Wien filter is about 40%, a 10^6 pps of the $^{22}Mg^{12+}$ secondary beam will be achieved by using the primary $^{20}Ne^{5+}$ current 350 pnA (2×10^{12} pps).

II.3. The observed reaction ^{22}Mg$(\alpha, p)^{25}$Al

The (α, p) reaction with the incident beam of ^{22}Mg will be performed at F3 scattering chamber in inverse kinematics. The central values and the energy ranges of Gamow windows in center of mass system of ^{22}Mg + α at different temperatures are showed in Table 1.

Table 1. Peaks and widths of Gamow energy window.

T_9 (GK)	$E_{0c.m}$ (MeV)	ΔE
1	1.52457	0.83703
2	2.42010	1.49142
3	3.17122	2.09094

The ^{4}He gas target and detectors for the experiment will be in a vacuum scattering chamber located at the end of the beam line. Two PPACs measured timing and position of the incoming ^{22}Mg beam with a resolution of about 1 mm. The timing signal is used for producing event triggers, and for particle identification using time-of-flight method. The position and incident angle of the beam at the target are determined by extrapolating the positions measured by PPACs. The ^{4}He target is a new gas cell of a semi-cylindrical shape, with a length of about 8 cm (given by the radius of the semi-cylinder). The entrance window is made of a havar foil of 2.5 μm thickness. The exit Mylar window is 25 μm thick. The cell will be filled with ^{4}He gas at 400 torr. The ^{4}He gas cell must be thick enough to stop all of beams, except protons. The energy loss in the center-of-mass system in the ^{4}He gas is estimated. It increases with low energy and could be compared with the energy resolution of the reaction 100 keV. The Fig. 6a shows the relationship between energy loss and energy of the (α, p) reaction in center-of-mass system. The energy loss of proton in laboratory system was estimated as shown in Fig. 6b.

The stacked silicon detectors (often called "telescopes") were also put inside the reaction chamber after the gas target to measure the energies of protons and charged particles. In this case, energies of recoiled protons up to 25 MeV can be measured. Each telescope consists of a position sensitive (16×16 stripped) detector with a thickness of 70 μm, and 2 or 3 layers of position-insensitive and 1.5 mm-thick detectors. The area is 50 mm×50 mm for all of them.

Five multi-layered silicon detector set, refers to as ΔE-E telescope, will be used for measuring the energy and angular distribution of the recoil protons. Each telescope

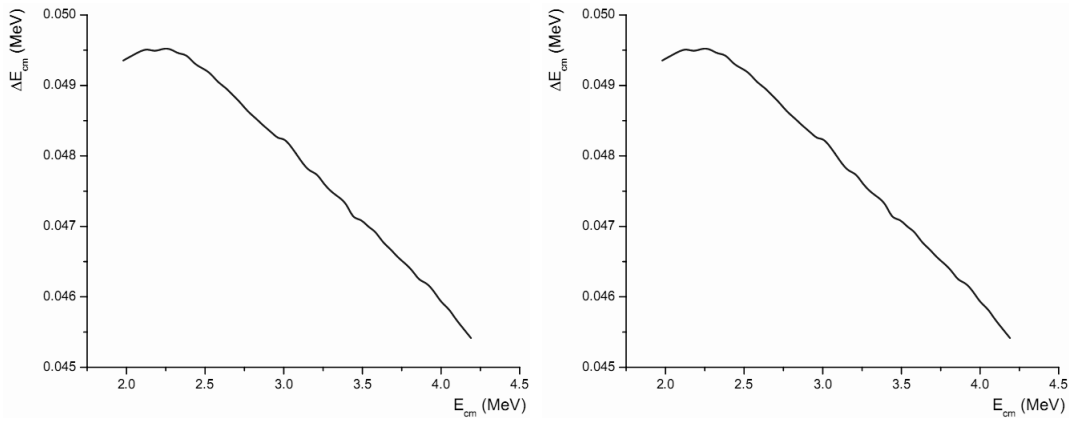

(a) (b)

Fig. 6. (a) The relationship between energy loss and reaction energy in gas target ^{4}He; (b) The energy loss of protons in gas target ^{4}He.

consists of a ΔE counter of 70 μm thickness following by an E counter of 1.5 mm thickness, all of which had an area of 50 mm×50 mm with 16×16 pixels [7]. It will be placed 15 cm from the target at 0^o. In this case, energies of recoiled protons up to 25 MeV can be measured. The maximum energy of the recoil protons in our case is about 13.62 MeV. Therefore, the telescopes are sufficiently thick to stop them. According to our simulation, the deviation energy of proton after reaction target is approximately $0.76 \div 0.88\%$. By using these ΔE-E telescopes, we are able to identify the recoil protons from other particles. The angular distribution of proton calculated by Lise++ with 0.59 MeV/u of ^{22}Mg is shown in Fig. 7a and Fig. 7b. The distribution is the maximum at 0^o and decrease with larger angle.

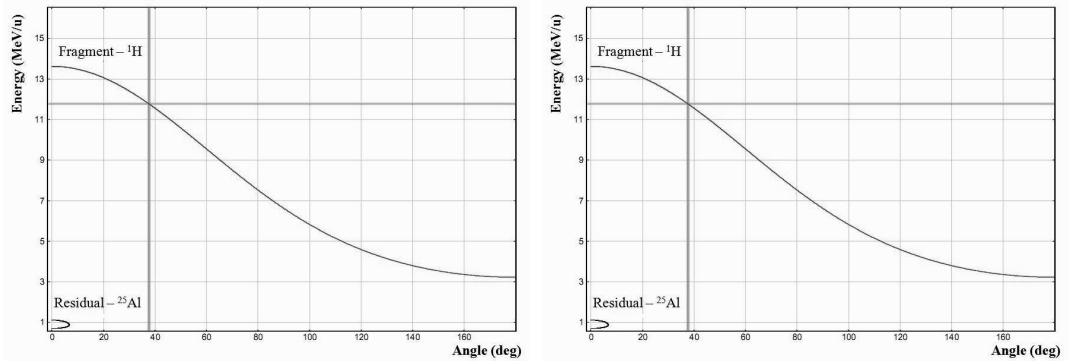

(a) (b)

Fig. 7. (a) The angular distribution of proton in laboratory system; (b) The angular distribution of proton in center-of-mass system.

One of our goals is scanning energy in region above alpha threshold of ^{22}Mg+α system (Q = 9.17MeV), which is still not completely known in the ^{26}Si levels scheme. Therefore, the energy of the incident beam ^{22}Mg must be in the range of E_x = 3.23 ÷ 3.29 MeV/u after production target (this value designed for energy of ^{22}Mg at center of observed reaction target about 0.49 ÷ 0.58 MeV/u). There are 4 open channels of the reaction ^{22}Mg+α at this energy range [9]. Other charge particles such as ^{24}Mg, ^{22}Mg, ^{25}Al do not have energy enough to pass through mylar-25μm exit window of secondary target so they cannot reach to the detector telescopes except the recoiled protons.

Reaction rate and cross section at the considered energy range were estimated by using NON-SMOKER code which bases on Hauser-Feshbach theory [21,22] and are presented in Table 2. The temperature higher, the reaction rate is larger. People believe that the synthesis will be vigorous if the X-ray burst environment has a high temperature.

Table 2. Reaction rate of ^{22}Mg(α,p)^{25}Al calculated by Hauser-Feshbach theory

T9 (GK)	E_{cm} (MeV)	Cross section (mb)	Reaction rate
1.0	1.52	0.0013	3.08740×10^{-5}
2.0	2.42	0.7710	1.27414
3.0	3.17	12.710	166.742

In order to estimate the expected yield, the value of cross section was calculated for a resonance at E_{cm} = 2 MeV by assuming contributions from an s-wave resonance at this energy with a width Γ_α near the Wigner limit. We also assume that the expected ^{22}Mg beam has intensity of about 2.5×10^5 pps. Under these assumptions, we obtained 2043 counts per energy bin of 67 keV at 0^o at this energy in 5 days, which corresponds to a statistical accuracy of 2%. According to prediction of cross section, the yield should be much higher respectively with higher energy as can be seen in Fig.9.

II.4. Main source of background and their elimination

Contaminants may come from production reaction such as ^{20}Ne, ^{18}Ne, ^{11}C, deuteron, proton, etc... They will be separated by D1, D2 magnets and Wien filter. After that, they can be eliminated using PPAC-PPAC to discriminate the beam ions by the time-of-flight method before reaching F3 target. The alpha particles from elastic scattering $\alpha(^{22}\text{Mg},\alpha)^{22}$Mg, other protons from the possible open channels, three-body reaction $\alpha(^{22}\text{Mg},2\text{p})^{24}$Mg, and from elastic scattering ^{4}He + p may reach to the detectors. They will be separated from interested protons in the F3 telescopes by ΔE-E method because the difference of energy. Background from the secondary beam in the PPAC and beam line typically appears as the high-energy protons from elastic scattering of the beam in these materials. As mentioned above, these high-energy protons can be distinguished from good events in the telescopes. Some protons might be collected by the accidental coincidence but they shoud be eliminated during off-line analysis because these events have no recoil trajectory. In order to eliminate contaminants from scattering in the havar foils, we will perform a background run by filling the target with a heavier gas, such as argon or xenon, at a pressure that gives an equivalent thickness in energy loss as the helium target.

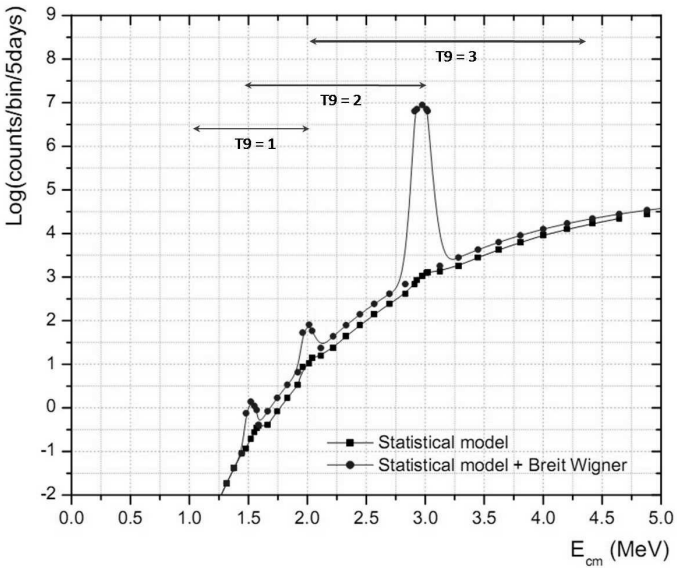

Fig. 8. The yield estimation as a function of the reaction energy in center of mass frame of ^{22}Mg + α system. The statistical estimation base on prediction of cross section in ref. [23].

III. CONCLUSION

The design for studying the stellar reaction ^{22}Mg(α,p)^{25}Al has been done based on simulation and experimental data of other works previously for (α,p) reaction with radioactive beam at CRIB. This design is necessary for experimental setup and for confirmation of the feasibility of the experiment.The cross sections of both production and secondary reaction are not known experimentally. Therefore, the intensity of the primary beam is still not precisely fixed. This will be verified by experiment. Our design has been accepted by Program Advisory Committee of RIKEN and CNS with very high priority. The beam time has been given for 15 days continuously by the committee. We are planning to perform a test experiment for 3 days in April of 2011 and the main experiment will be performed after adjusting the setup by using the experimental results. The design expected to be useful to setup the experiment successfully.

ACKNOWLEDGEMENT

The authors would like to thank our consultant in this work, Prof. S.Kubono, for his interest, guidance and support. This work was partial financial sponsored by the Vietnam's National Foundation for Science and Technology Development (NAFOSTED) under Contract No. 103.04.54.09.

REFERENCES

[1] E. M. Burbidge, G. Burbidge,W. A. Fowler, and F. Hoyle, *Rev. Mod. Phys.* **29** (1957) 547.
[2] A. G. W. Cameron, *Atomic Energy of Canada, Ltd.*, CRL-41 (1957).

[3] A. Unsold, *Science* **163** (1969) 1015.
[4] G. Wallerstein, *ibid.* **162** (1968) 625.
[5] J. L. Fisker and F. K Thielemann, *The Astrophysical Journal* **608** (2004) L61–L64.
[6] J. Jose, A. Coc, and M. Hernamz, *The Astrophysical Journal* **520** (1999) 347–360.
[7] S. Kubono, *Nucl. Inst. and Meth.* **A539** (2005) 74–83.
[8] David Miles Kahl, *^{30}S Beam Development and the ^{30}S Waiting Point in Type I X-Ray Bursts*, http://physwww.physics.mcmaster.ca/∼chenal/nuc_astro_struc/group/home/theses.html.
[9] http://t2.lanl.gov/data/qtool.html.
[10] N. Bateman *et al.*, *Phys. Rev.* ***C*63** (2001) 035803.
[11] R. A. Paddock, *Phys. Rev.* **C5** (1972) 485.
[12] A. A. Chen *et al.*, *Phys. Rev.* **C63** (2001) 065807.
[13] C. Jewetta *et al.*, *Nucl. Inst. and Meth. Physics in Research* **B261** (2007) 945–947.
[14] A. B. McDonald and E. G. Adelberger , *Nuclear Physics* **A144** (1970) 593 - 606.
[15] R. E. Benenson and I. J. Taylor, *Nuclear Physics* **A197** (1970) 305 - 314 .
[16] S. K. Bose, A.Kogan, and P. R. Bevington, *Nuclear Physics* **A219** (1974) 115 - 124.
[17] W. P. Alford *et al.*, *Nuclear Physics* **A457** (1986) 317-336.
[18] H. Kumagai *et al.*, *Nucl. Inst. and Meth.* **A470** (2001) 562.
[19] C.E. Rolfs and W. S. Rodney, *Cauldrons in the Cosmos*, the University of Chicago Press, 1988.
[20] S.I. Sukhoruchkin and Z.N. Soroko, *Energy Levels and Branching Ratios for Si-26 (Silicon-26).* http://www.springerlink.com/content/th3qw7h0m1n4l106/
[21] http://www-astro.ulb.ac.be/Nucdata/Talys/acapMG.
[22] Christian Iliadis, *Nuclear Physics of Stars*, Wiley-VCH Verlag, p. 141-146.
[23] T. Rausher *et al.*, *Atomic Data Nuclear Data Tables* **75** (2000) 1 and **79** (2001) 47.

Received 25 August 2010.